OPEN

Downregulated miR-45 Inhibits the G1-S Phase Transition by Targeting Bmi-1 in Breast Cancer

Lan Wang, Jun-Ling Liu, Liang Yu, Xiang-Xia Liu, Hong-Mei Wu, Fang-Yong Lei, Shu Wu, and Xi Wang

Abstract: Bmi-1 (B cell-specific Moloney murine leukemia virus integration site 1) is upregulated in breast cancer and was involved in many malignant progressions of breast cells, including cell proliferation, stem cell pluripotency, and cancer initiation. However, the epigenetic regulatory mechanism of Bmi-1 in breast cancer remains unclear.

After analysis of the ArrayExpress dataset GSE45666, we comparatively detected the expression levels of miR-495 in 9 examined breast cancer cell lines, normal breast epithelial cells and 8 pairs of fresh clinical tumor samples. Furthermore, to evaluate the effect of miR-495 on the progression of breast cancer, MCF-7 and MDA-MB-231 were transduced to stably overexpress miR-495. The 3-(4,5-dimethyl-2-thiazolyl)-2,5-diphenyl-2-H-tetrazolium bromide assay, colony formation assays, 5-Bromo-2-deoxyUridine labeling and immunofluorescence, anchorage-independent growth ability assay, flow cytometry analysis, and luciferase assays were used to test the effect of miR-495 in MCF-7 and MDA-MB-231 cells *in vitro*. Xenografted tumor model was also used to evaluate the effect of miR-495 in breast cancer.

Herein, we found that miR-495, a predicted regulator of Bmi-1, was frequently downregulated in malignant cells and tissues of breast. Upregulation of miR-495 significantly suppressed breast cancer cell proliferation and tumorigenicity via G1-S arrest. Further analysis revealed that miR-495 targeted Bmi-1 through its 3′ untranslated region. Moreover, Bmi-1 could neutralize the suppressive effect of miR-495 on cell proliferation and tumorigenicity of breast cancer *in vivo*.

These data suggested that miR-495 could inhibit the G1-S phase transition that leads to proliferation and tumorigenicity inhibition by targeting and suppressing Bmi-1 in breast cancer.

Editor: Namrata Bhatnagar.
Received: November 13, 2014; revised: March 8, 2015; accepted: March 9, 2015.
From the Department of Pathogen Biology and Immunology, School of Basic Courses, Guangdong Pharmaceutical University (LW, H-MW); Department of Medical Oncology, Sun Yat-sen University Cancer Center (JLL); Department of Vascular and Breast Surgery, the First Affiliated Hospital of Sun Yat-sen University, Guangzhou (LY); Department of Plastic Surgery, the First Affiliated Hospital of Sun Yat-sen University (X-XL); State Key Laboratory of Oncology in South China (F-YL, SW); State Key Laboratory of Oncology in Southern China, Department of Experimental Research, Sun Yat-sen University Cancer Center, Guangzhou, Guangdong, China (XW).
Correspondence: Lan Wang, Department of Pathogen Biology and Immunology, School of Basic Courses, Guangdong Pharmaceutical University, Guangzhou 510006, China (e-mail: wanglan3435@hotmail.com).
Xi Wang, Department of Experimental Research, Sun Yat-sen University Cancer Center, Guangzhou, Guangdong 510060, China (e-mail: 1272908565@qq.com).
This study was supported by the National Natural Science Foundation of China (Grants: 81201677, 81201548, 81201546 and 81171892).
The authors have no conflict of interest.

ISSN: 0025-7974
DOI: 10.1097/MD.0000000000000718

(*Medicine* 94(21):e718)

Abbreviations: 3′ UTR = 3′-untranslated region, AKT = v-akt murine thymoma viral oncogene homolog 1, Bmi-1 = B-cell-specific Moloney murine leukemia virus integration site 1, GFI1 = growth factor independent 1 transcription repressor, GFP = green fluorescent protein, H&E = hematoxylin-eosin staining, miRNA = microRNA, mut = mutant, NBEC = normal breast epithelial cell, NFκB = nuclear factor kappa B, PBS = phosphate buffer saline, PTEN = phosphatase and the tensin homolog deleted on chromosome 10, Rb = retinoblastoma 1, wt = wild-type.

INTRODUCTION

Bmi-1, a polycomb group protein, was originally identified as a transgene that could co-operate with c-Myc (v-myc avian myelocytomatosis viral oncogene homolog) to induce hematopoietic malignancies,[1] and acts as master switch for cell proliferation,[2] early embryogenesis,[3] stem cell pluripotency,[4] and cancer initiation.[5] Bmi-1 is necessary for the progression of many types of cancer, and increased Bmi-1 expression may contribute to tumorigenesis, such as in hepatocellular carcinoma,[6] oral squamous cell carcinoma,[7] small-cell lung cancer,[8] and gastric cancer.[9] Nacerddine reported that Bmi-1 showed its oncogenic potential, E3 ligase activity, and DNA damage repair activity in mouse prostate cancer.[10] Downregulation of the *Bmi-1* gene by RNAi inhibited the proliferation and invasiveness of breast cancer cells and laryngeal carcinoma cells.[4,11]

The clinicopathological characteristics of Bmi-1 indicated its significance in clinical diagnosis and potential therapy.[4,12] Hayry et al[13] reported that Bmi-1 is an independent marker for poor prognosis in oligodendroglial tumors. Bmi-1 expression displayed a significant inverse association with patient overall survival ($P = 0.006$) and mean survival ($P < 0.001$).[4] A high level of Bmi-1 indicates unfavorable overall survival and serves as a high-risk marker for breast cancer.[14] Song et al[15] found that Bmi-1 transcriptionally downregulated the expression of the tumor suppressor *PTEN* in tumor cells through direct association with the PTEN locus. *Sp1* and *c-Myc* were observed to regulate the transcription of Bmi-1 in nasopharyngeal carcinoma in tumor sample;[16] VEGF/neuropilin-2 regulation of Bmi-1 defines a novel mechanism of aggressive prostate cancer.[17] In a recent study, Jiang et al[18] revealed the Bmi-1 was involved in the nuclear factor kappa B (NFκB) pathway. However, an epigenetic regulatory mechanism for the overexpression of Bmi-1 in breast cancer has not been fully clarified.

MicroRNAs (miRNAs) are proven to inhibit gene translation or facilitate mRNA degradation, resulting in repression of target genes expression.[19] According to miRBase, >1000 different mature miRNAs have been identified in human.[20] As important epigenetic regulators, miRNAs have vital roles in cancer

progression.[21] Many miRNAs function as oncogenes, such as miR-34a,[22] miR-320,[23] and miR-21,[24] whereas the others function as tumor suppressor genes such as miR-154,[25] miR-126,[26] and miR-203.[27] MiRNAs are involved in many important signal pathways, such as the TGFβ pathway,[28] AKT pathway[29] and WNT pathway.[30] MiR-22 overexpression induces phosphatase and tensin homolog (PTEN) downregulation and phosphoinositide 3-kinase (PI3K)/AKT pathway activation.[31] MiR-7 inhibits tumor metastasis and reversed the epithelial-mesenchymal transition through AKT and ERK1/2 pathway inactivation.[32]

Here, we reported that miR-495 was frequently downregulated in malignant cells and tissues of breast. Upregulation of miR-495 significantly suppressed breast cancer cell proliferation, possibly through G1-S arrest. We demonstrated that miR-495 directly targeted the 3′-untranslated region (3′ UTR) of the *Bmi-1* mRNA and regulated the expression of PTEN, $p21^{Cip1}$and $p27^{Kip1}$, cyclin D1, and phosphorylated AKT. In vivo xenograft formation assays supported the phenotype observed with miR-495-transfected cells and Bmi-1 replenished cells. Our results suggest that frequent downregulation of miR-495 in breast cancer may influence the G1-S phase transition by targeting Bmi-1.

METHODS

Cell Culture

Normal breast epithelial cells (NBECs), breast cancer cell lines, and stably transfected cells were maintained according to our previous report.[33]

Real-time Polymerase Chain Reaction

The mirVana miRNA Isolation Kit (Ambion, Austin, TX), the Taqman miRNA reverse transcription kit (Applied Biosystems, Foster City, CA), the miRNA-specific TaqMan MiRNA Assay Kit (Applied Biosystems, Foster City, CA) and the Applied Biosystems 7500 Sequence Detection system were used to perform real-time quantitative polymerase chain reaction (PCR) as previously described.[34] The primers used were as follows: Bmi-1, forward, 5′-TCGTTGTTCGATGCATTTCT-3′, and reverse, 5′-CTTTCATTGTCTTTTCCGCC-3′; $p21^{Cip1}$, forward, 5′-CGAT GCCAACCTCCTCAACGA-3′, and reverse, 5′-TCGCAGAC CTCCAGCATCCA-3′; $p27^{Kip1}$, forward, 5′-TGCAACCGACG ATTCTTCTACTCAA-3′, and reverse, 5′-CAAGCAGTGATGT ATCTGATAAACAAGGA-3′; cyclin D1, forward, 5′-AAC TA CCTGGACCGCTTCCT-3′, and reverse, 5′-CCACTT GAGC TTGTTCACCA-3 GAPDH, forward, 5′-GACTCATGACCAC AGTCCATGC-3′, and reverse, 3′-AGAGGCAGGGATGATG TTCTG-5′.

Plasmid and Transfection

The only 1 miR-495 binding site of Bmi-1 3′ UTR is from 326 base pairs (bp) to 333 bp. The 230 bp-length sequence of human Bmi-1–3′ UTR (from 204 to 453) was cloned into the pGL3-basic luciferase reporter plasmid (Promega, Madison, WI) and pGFP-C3 (Clontech, Mountain View, CA).[34] The p3xIRS-MLP-luc plasmid, pMSCV/Bmi-1(with 3′ UTR or without 3′ UTR), and pMSCV /miR-495 were constructed as previously described.[34–36] The primers selected were as follows: miR495-up: 5′-GCCAGATCTGCTTTATCCGTCATGACTGT-3′; miR4 95-dn: 5′-GCCGAATTCTGGCTGCTATGATCTGAACT-3′; Bmi-1–3′ UTR-wt-up: 5′-GCCCCGCGGGAATTGGTTTCT TGGAAAGCAG-3′; Bmi-1–3′ UTR-wt-dn: 5′-GCCCTGCA-GATGCATATTCTTTCCGTTGG-3′; Bmi-1–3′ UTR-mut-up: 5′-TAAGCATTGGGCCATAGTTTCAAAATCTCAACTAACG CCTACATTACATTCTCC-3′; Bmi-1–3′ UTR-mut-dn: 5′-GGA GAATGTAATGTAGGCGTTAGTTGAGATTTTGAAACTATG GCCCAATGCTTA-3′.

Western Blot

Western blot analysis was performed as previously described,[33] using anti-α-tubulin, anti-Bmi-1(Millipore, Billerica, MA), anti-p21, anti-p27, anti-cyclin D1, anti-Rb, anti-phosphorylated Rb (Abcam, Cambridge, MA), anti-PTEN, anti-AKT, anti-phosphorylated AKT^{Thr308} and anti-phosphorylated AKT^{Ser473} (Sigma, St. Louis, MO) antibodies.[34]

3-(4, 5-dimethyl-2-thiazolyl)-2, 5-diphenyl-2H-tetrazolium Bromide Assay

Ninety-six-well plates were used to culture 1×10^4 cells each hole and all experiments were performed in triplicate as to our previous report.[33,34]

Colony Formation Assays

Five hundred cells per plate were incubated on 6-well plates for 10 days. The colonies were fixed, stained, and counted as to our previous report.[33,34]

Anchorage-independent Growth Ability Assay

Five hundred cells/well were seeded, counted, and measured according to our previous report.[33,34]

5-Bromo-2-deoxyuridine Labeling and Immunofluorescence

The images of cells stained with anti-5-bromo-2-deoxyuridine (BrdUrd) antibody (Upstate, Temecula, CA) after incubation with BrdUrd for 1 h were acquired by a laser scanning microscope (Axioskop 2 plus, Carl Zeiss Co. Ltd.).[34]

Flow Cytometry Analysis

According to previous report,[34] 20,000 harvested cells were washed, fixed, pelleted, re-suspended, incubated with bovine pancreatic RNAase (Sigma, Saint Louis, MO), and stained with propidium iodide (Sigma-Aldrich) before analyzed on a flow cytometer (FACSCalibur; BD Biosciences).[34]

Luciferase Assays

According to the manufacturer's recommendation of the Lipofectamine 2000 reagent (Invitrogen Co, Carlsbad, CA), 100 ng of p3x IRSMLP -luciferase plasmid, or pGL3-Bmi-1–3′ UTR (wt/mut), or the control-luciferase plasmid, plus 1ng of pRL-TK renilla plasmid (Promega, Madison, WI) was transfected into the indicated cells.[34] The Dual Luciferase Reporter Assay Kit (Promega, Madison, WI) was used to detect luciferase and renilla signals 48 h after transfection.[34]

Xenografted Tumor Model, Immunohistochemistry, and Hematoxylin and Eosin Staining

BALB/c-nu mice (4–5 weeks of age, 18–20 g) were purchased from Hunan SJA Laboratory Animal Co, Ltd, Hunan, PR China. According to our previous report, the BALB/c nude mice were randomly divided into 2 groups (5 per group): the first group was inoculated in situ with MDA-MB-231-NC cells (5×10^6) in the left breast and with MDA-MB-231-miR-495 cells(5×10^6) in the right breast per mouse; the second group was inoculated in situ with MDA-MB-231–495-Bmi-1-vector cells (5×10^6) in the left

breast and with MDA-MB-231–495-Bmi-1-ORF cells (5×10^6) in the right breast per mouse.[37] Tumors were measured and calculated every 3 days until the 37th day. The acquired tumors were subjected to immunohistochemistry using an anti-Bmi-1 antibody (1:500; Upstate, Temecula, CA) or hematoxylin-eosin (H&E) stain with Mayer hematoxylin solution. The Institutional Animal Care and Use Committee of Sun Yat-sen University approved all the experimental procedures.

Statistical Analysis

Student *t* test in SPSS13.0 (IBM, Armonk, NY) was used to evaluate the significant difference of 2 groups of data in all the pertinent experiments. A P value <0.05 (using a 2-tailed paired *t* test) was considered statistically significant.[33,34]

RESULTS

MiR-495 Expression is Downregulated in Breast Cancer

Analysis of the ArrayExpress dataset GSE45666 indicated that miR-495 expression was frequently decreased in 101 breast cancer tissues compared with 15 adjacent noncancerous breast tissues. Among the 101 cancer samples, the expression of miR-495 in 99 samples was lower than the mean of the 15 adjacent noncancerous breast tissues (Figure 1A). The details of these 116 samples are listed in the supplementary Table 1, http://links.lww.com/MD/A245 (see table, supplemental content, http://links.lww.com/MD/A245, which illustrates the detail information of the samples). Further analysis showed that miR-495 expression is significantly decreased in 10 tissues and slightly decreased in 3 tumor tissues (a total of 15 pairs) compared with their adjacent noncancerous tissues in GSE45666 ($P < 0.001$) (Figure 1B). As compared with NBEC, real-time PCR analyses revealed that miR-495 was significantly downregulated in all 9 examined cell lines (changing fold was from 3% to 33%, Figure 1C). To further confirm these differences, comparative analysis of expression of miR-495 was conducted by real-time PCR. As shown in Figure 1D, miR-495 was downregulated in malignant tumor samples compared with the paired adjacent tissues (Figure 1D). Taken together, these data revealed that miR-495 expression is frequently downregulated in breast cancer.

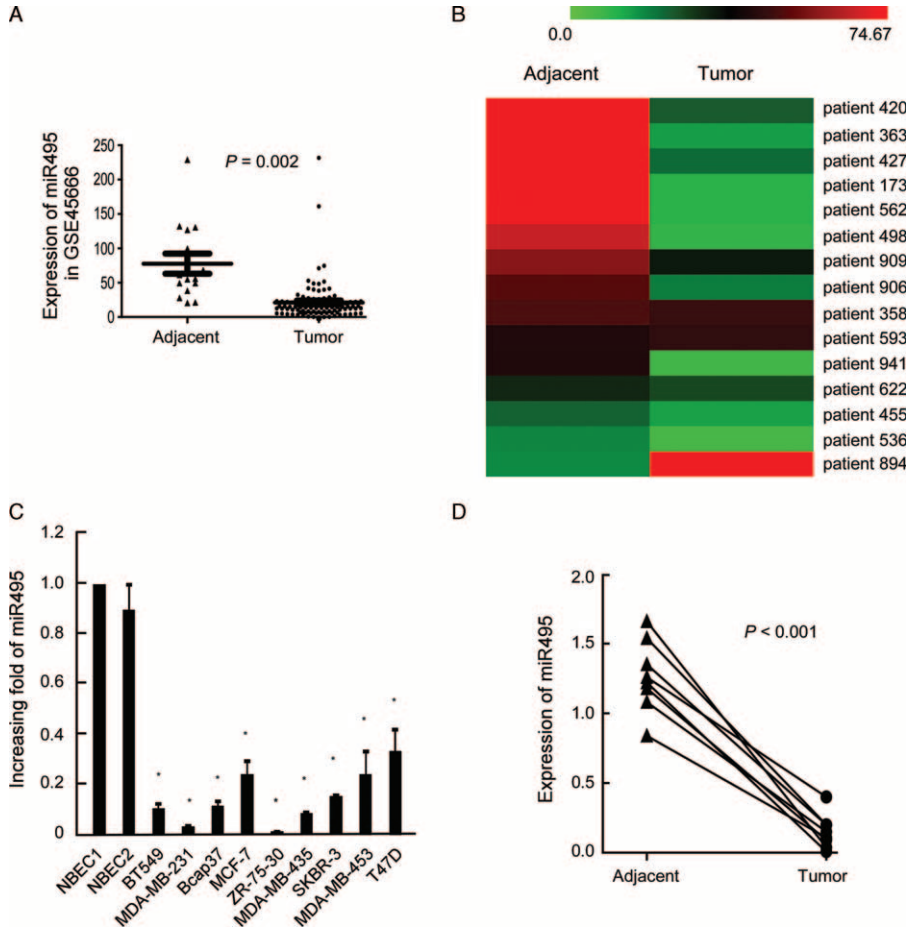

FIGURE 1. The expression of miR-495 in breast cancer. (A) The expression of miR-495 was frequently downregulated in 101 breast tumor tissues (Tumor) compared with 15 adjacent noncancerous breast tissue samples (Adjacent) in the GSE45666 dataset. (B) MiR-495 expression was markedly reduced in 15 paired breast tumor tissues (Tumor) and their adjacent noncancerous tissues (Adjacent) in the GSE45666 database. (C) Real-time PCR analysis of miR-495 expression in indicated cells. (D) The expression of miR-495 in eight collected fresh tumor tissues (Tumor) and their adjacent noncancerous tissues (Adjacent). *U6* was used as the normalized gene. Three independent experiments were conducted in each assay.

Overexpression of miR-495 Suppresses Proliferation

To examine the effect of miR-495 on the progression of breast cancer, breast cancer cells MCF-7 and MDA-MB-231 stably overexpressing miR-495 were established (Figure 2A). 3-(4, 5-dimethyl-2-thiazolyl)-2, 5-diphenyl-2H-tetrazolium bromide (MTT) assays showed that miR-495-transfected cells had a significant decrease in the growth rate compared with that of negative-control-transduced cells (NC) (Figure 2B). The results showed that 421 colonies were present in miR-495-transfected MCF-7 cells, compared with the 112 colonies in NC-transfected MCF-7. The same trend was found in the MDA-MB-231 cells (Figure 2C). As Ki-67 is considered to be a proliferation marker, the staining of Ki-67-positive cells was employed to detect the rapidly proliferating cells.[38] As the Figure 2D shown, the proportion of Ki-67-positive cells was dramatically decreased in miR-495-transfected MCF-7 and MDA-MB-231 cells, further suggesting that upregulation of miR-495 suppressed the proliferation of breast cancer cells. Moreover, colony number and size were both decreased in miR-495-transfected MCF-7 and MDA-MB-231 cells, further supporting the suppressive effect of miR-495 on proliferation in breast cancer cells (Figure 2E).

MiR-495 Inhibits the G1-S Phase Transition

We further investigated the mechanism by which miR-495 suppressed cell proliferation. Flow cytometry analyses revealed that miR-495 could reduce the proportion of cells entering S phase and increase the proportion of cells staying at G1/G0 phase. The results showed that 66.93% G1/G0 phase cells and only 17.03% S phase cells were present in miR-495-transfected MCF-7 cells, compared with the 53.17% G1/G0 phase cells and

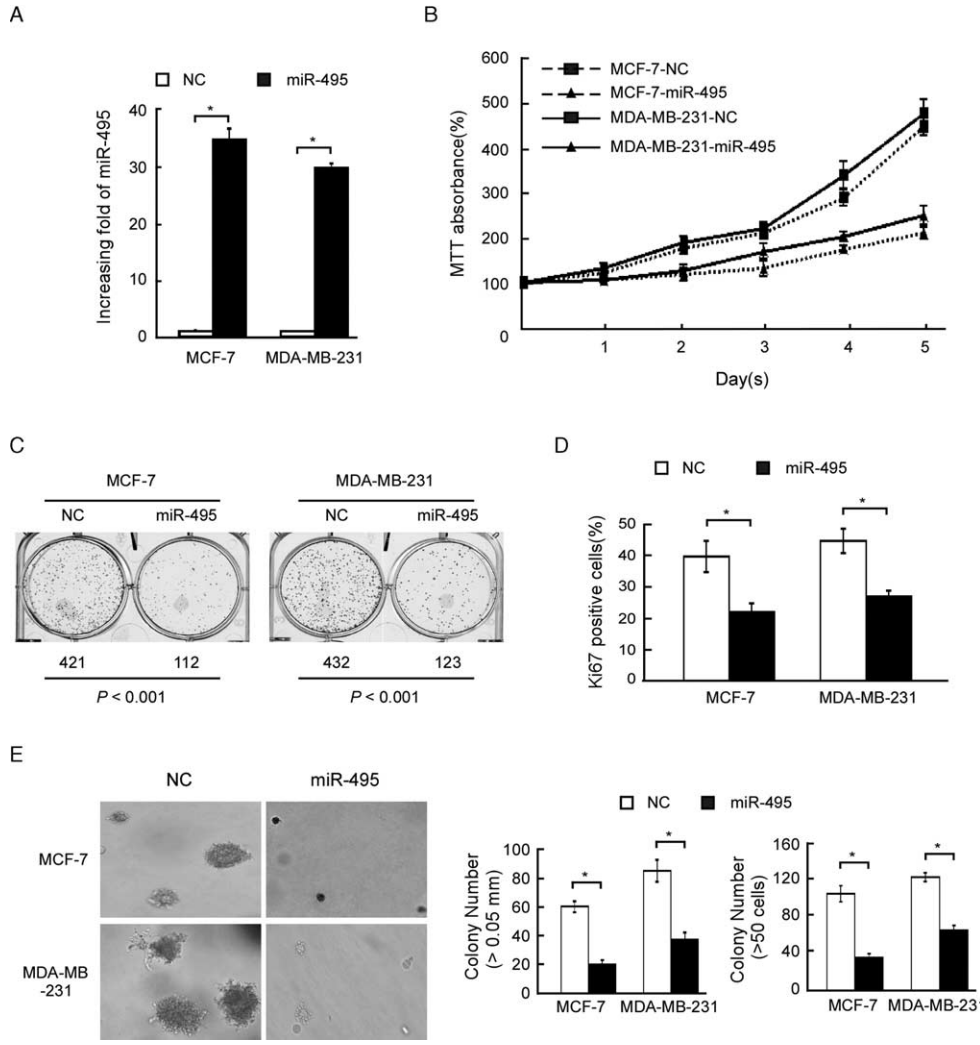

FIGURE 2. The effect of miR-495 on the proliferation and tumorigenicity of breast cancer cells MCF-7 and MDA-MB-231. (A) Increasing levels of miR-495 expression as assessed by real-time PCR. (B) MTT assays showing that miR-495-transfected cells grow slower than the NC-transfected cells. (C) Representative micrographs and quantification of formative colonies (MCF-7-NC, MCF-7-miR-495, MDA-MB-231-NC, MDA-MB-231-miR-495), which were crystal violet-stained. (D) The proportion of Ki-67 positive cells in cells transfected with miR-495 decreased. (E) Representative micrographs (left) and numbers of colonies in the anchorage-independent growth assay. Three independent experiments were conducted in each assay. $^{*}P < 0.05$. MTT = 3-(4, 5-dimethyl-2-thiazolyl)-2, 5-diphenyl-2H-tetrazolium bromide.

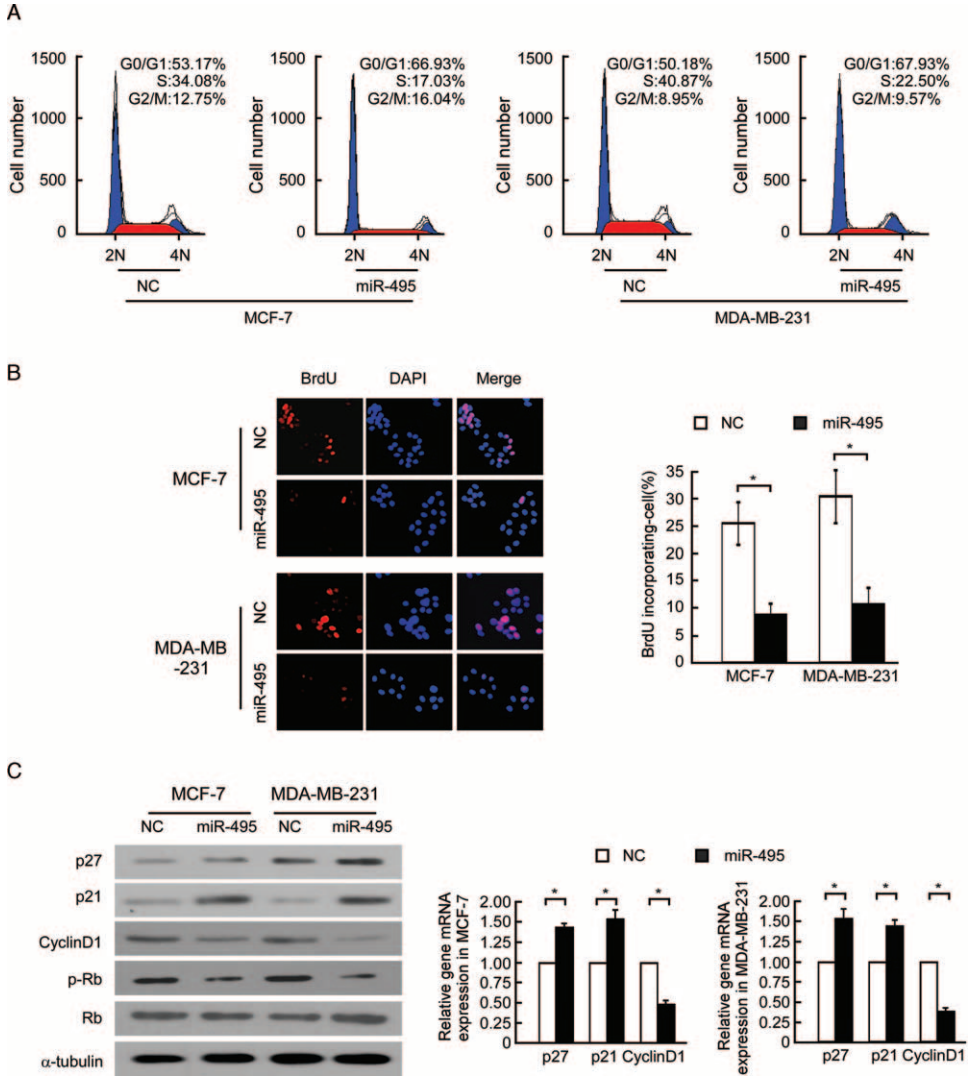

FIGURE 3. The inhibitory role of miR-495 in the G1-S phase transition. (A) Obvious changes in the percentage of cells in the G1/G0 peak or S peak in miR-495-transfected breast cancer cells was detected by the flow cytometry analysis. (B) Representative micrographs (left) and quantification (right) of BrdUrd incorporating cells indicated miR-495-mediated proliferation inhibition. (C) The protein expression and mRNA levels of indicated cell-cycle-associated genes were tested by real-time PCR and western blot analysis. GAPDH and α-tubulin were used as a loading controls, separately. $^{*}P < 0.05$.

34.08% S phase cells in NC-transfected MCF-7. Similar results were found in the MDA-MB-231 cells (Figure 3A). Furthermore, BrdUrd incorporation assay showed a markedly decreased percentage of newly synthesized DNA in miR-495-transfected MCF-7 cells (9.15%) and miR-495-transfected MDA-MB-231 cells (11.01%) compared with NC-transfected cells (26.04% in MDA-MB-231; 31.12% in MCF-7) (Figure 3B). Collectively, our data suggested that the suppressive effect of miR-495 on breast cancer cell growth probably attributes to the G1-S transitional arrest.

MiR-495 Modulates Cell-cycle Regulators

Cell cycle is verified to be modulated by many cell-cycle promotors and inhibitors, such as Rb and cyclin D1 in the regulation of the G1/S transition.[39,40] Compared with the NC-transfected cells, the protein and mRNA expressions of $p21^{Cip1}$ and $p27^{Kip1}$, 2 cell-cycle inhibitors, were increased in miR-495-transfected cells. However, the expression of cyclin D1, a cell-cycle promoter, was decreased in miR-495-transfected cells. The phosphorylation level of Rb, positively correlating with cell-cycle, was dramatically decreased in miR-495-transfected cells (Figure 3C). These results further suggested that miR-495 inhibits the G1-S transition in breast cancer cells.

MiR-495 Directly Targets the Oncogene Bmi-1

We screened 3 publicly algorithms (Pictar, miRANDA, and TargetScan) searching for a potential target gene of miR-495. As shown in Figure 4A, diagrammatic sketch of predicted consequential pairing of target region and miRNA indicated that *Bmi-1* is a potential target gene of miR-495. In consideration of the effects of miRNAs on repression of target genes expression, we detected the predicted Bmi-1 gene expression by western

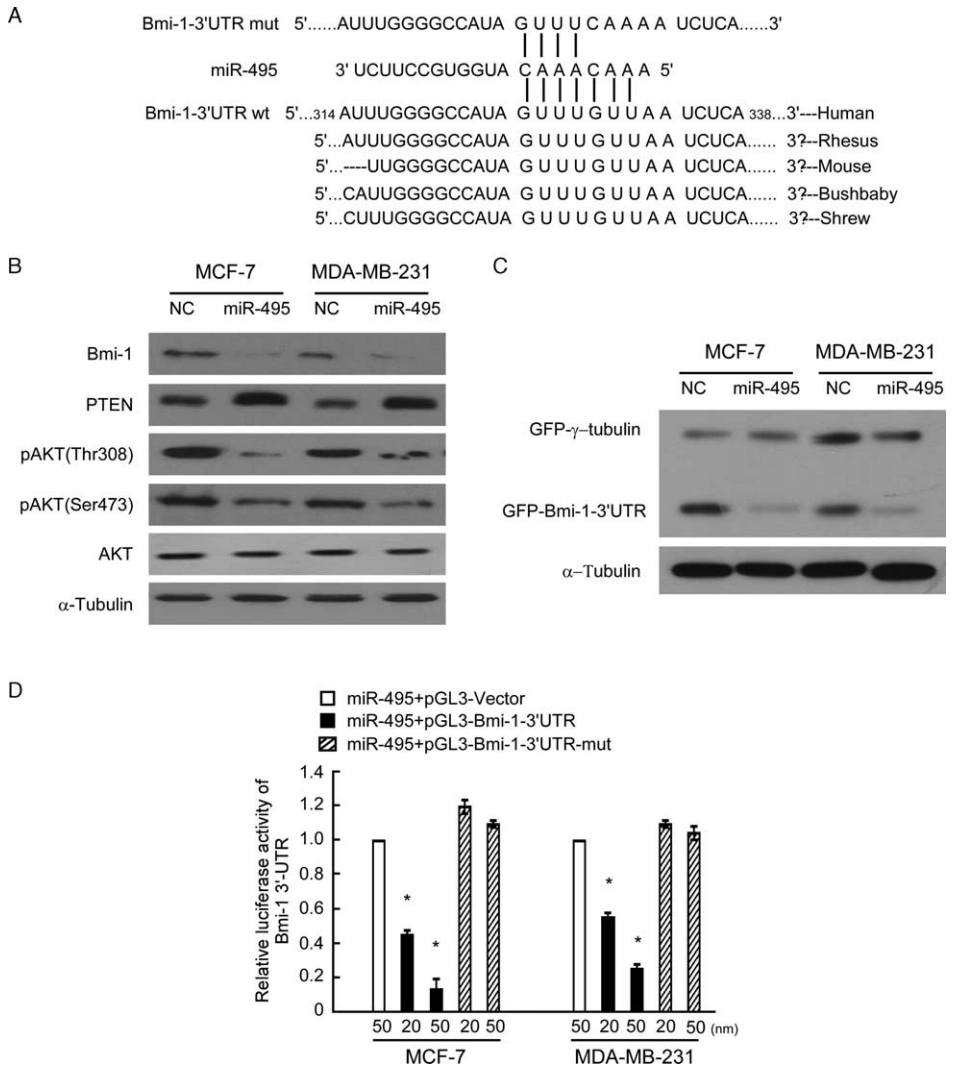

FIGURE 4. MiR-495 directly targeting the *Bmi-1*-3′ UTR. (A) Diagrammatic sketch indicated the miR-495 target sequences (wt: wild-type; mut: mutant) in the 3′ UTR of *Bmi-1* (B) Western blot analysis of Bmi-1, PTEN, p-AKT$^{(Thr308)}$, p-AKT$^{(Ser473)}$, and total AKT expression in indicated cells. (C) Western blotting analysis of GFP expression in the indicated cells. (D) The luciferase activity of Bmi-1-3′ UTR was tested in the indicated cells with increasing amounts of miR-495 plasmid (20 nmol/L, 50 nmol/L). Error bars correspond to the mean ± standard deviation. $^{*}P < 0.05$. UTR = untranslated region.

blot. Western blot revealed that ectopic expression of miR-495 in MCF-7 and MDA-MB-231cells reduced the expression of the Bmi-1 protein (Figure 4B). *AKT*, a gene typically affected by Bmi-1, showed changes in its phosphorylation levels consistent with reduced Bmi-1 expression (Figure 4B). PTEN, a tumor suppressor included in the AKT pathway, was upregulated in miR-495-transfected cells (Figure 4B). Furthermore, plasmids of Bmi-1 3′ UTR fragment containing predicted sequences (vectors are pEGFP-C3 and pGL3) were transfected in MCF-7 and MDA-MB-231 cells. As shown in Figure 4C, the expression of the GFP protein, but not the expression of GFP-γ-tubulin, was dramatically decreased in miR-495-transfected cells compared with in the NC-transfected cells. These data indicated an immediate relevance between miR-495 and Bmi-1−3′ UTR. Luciferase activity was also reduced in miR-495-transfected cells in a dose-dependent manner. Nevertheless, the mutation in the specific region of Bmi-1−3′ UTR (GUU to CAA) abrogated the inhibitory effect of miR-495 (Figure 4A and D). Taken together, we concluded that Bmi-1 is a genuine target of miR-495.

Bmi-1 is Intimately Involved in miR-495-induced G1-S Arrest of Breast Cancer Cells

To determine the role of Bmi-1 in miR-495-mediated G1-S arrest, the plasmids of Bmi-1 open reading frame (ORF, without the 3′ UTR), and Bmi-1−3′ UTR (ORF with the 3′ UTR) were created and used to process miR-495-transfected cells. As expected, overexpressing Bmi-1-ORF, but not Bmi-1−3′ UTR, could indeed dramatically reduce the expression of $p21^{Cip1}$/ $p27^{Kip1}$ and increase the expression of cyclin D1, suggesting an obvious attenuated effect of Bmi-1-ORF on the modulation of cell-cycle regulators by miR-495 overexpression (Figure 5A). Consistently, ectopically expressing Bmi-1-ORF, but not Bmi-1-3′ UTR, could rescue the luciferase activity of Bmi-1 reporter modulated by miR-495 (Figure 5B).

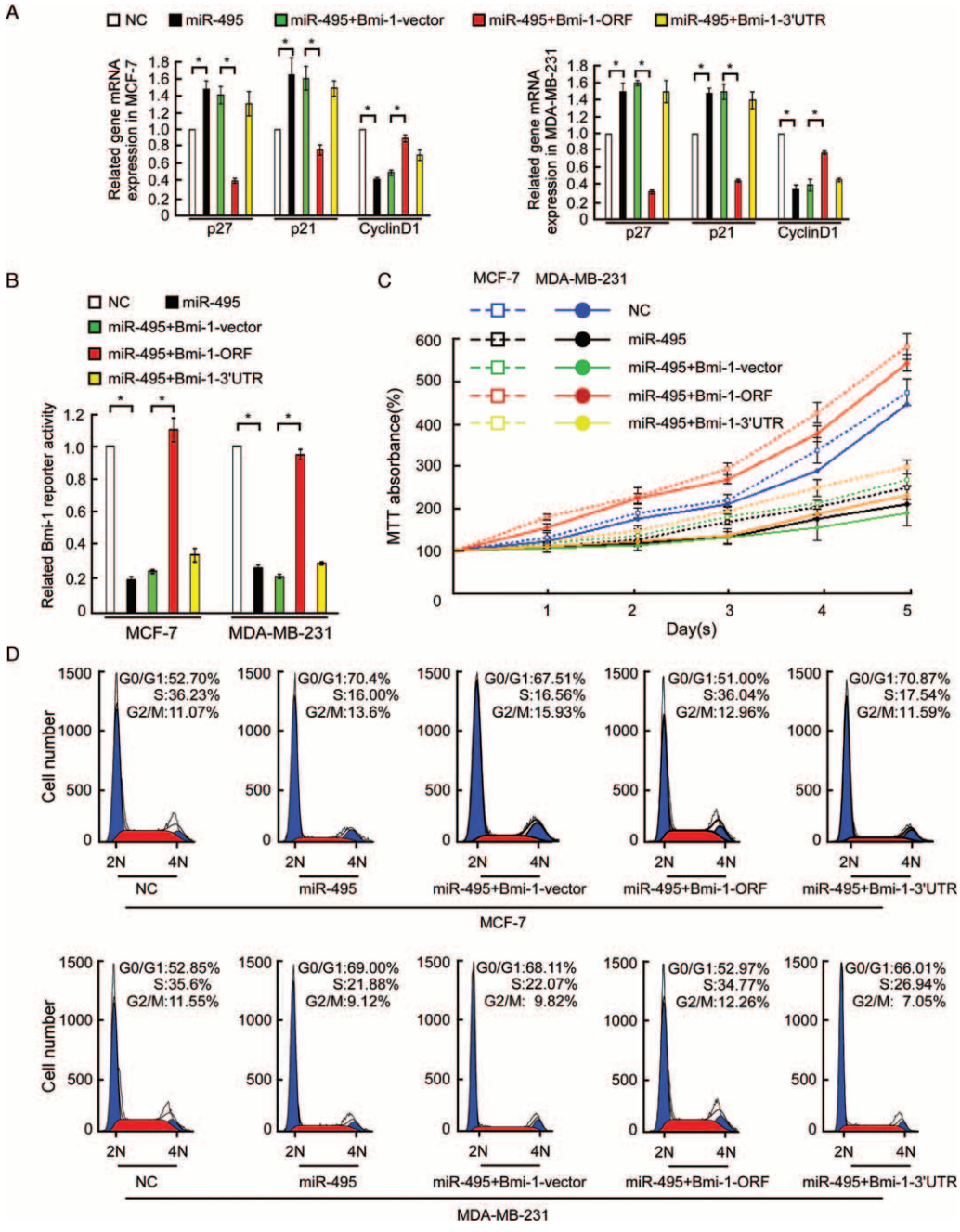

FIGURE 5. The role of Bmi-1 replenishment in miR-495-induced G1-S arrest. (A) Real-time PCR analysis of the expression of indicated genes in MCF-7 (left) or MDA-MB-231 (right) cells. GAPDH was used as a loading control. (B) The luciferase activities of Bmi-1 reporter were tested in indicated cells. (C) MTT assays revealed the growth rate of breast cancer cells transfected with NC, miR-495, or mixed miR-495 and Bmi-1-ORF (without 3′ UTR), or mixed miR-495 and Bmi-1-3′ UTR (ORF + 3′ UTR). (D) Flow cytometry analysis of indicated breast cancer cells. MTT = 3-(4, 5-dimethyl-2-thiazolyl)-2, 5-diphenyl-2H-tetrazolium bromide, UTR = untranslated region.

Furthermore, we investigated the effect of Bmi-1-ORF or Bmi-1-3′ UTR on the growth rate in the miR-495-transfected cells by the MTT assay. As shown in the Figure 5C, only Bmi-1-ORF dramatically accelerated the proliferation of miR-495-transfected cells. Meanwhile, flow cytometry showed that only co-transfection of miR-495 and Bmi-1-ORF dramatically increased the S phase percentage of MCF-7 and MDA-MB-231 cell lines (Figure 5D). These results indicated that Bmi-1 is intimately involved in miR-495-induced G1-S arrest of breast cancer cells.

The Relationship Between miR-495 and Bmi-1 Pathway Is Verified in Clinical Breast Samples

Human primary tumor samples were used to further confirm the above conclusion according to researches in subculture breast cancer cells. The expression levels of miR-495, Bmi-1, $p21^{Cip1}$,

$p27^{Kip1}$, and cyclin D1 were examined in 8 paired noncancerous human breast tissues (N1–N8) and breast tumor tissues (T1–T8). Colors in Figure 6 depict the expression of indicated genes tested by real-time PCR (red represents higher expression; green represents lower expression). The correlation coefficient and significance between miR-495 and indicated genes were listed in Figure 6. MiR-495 expression was negatively correlated with Bmi-1 ($r = -0.802$, $P < 0.001$) and cyclin D1 ($r = -0.729$, $P = 0.001$), whereas it was positively correlated with $p21^{Cip1}$ ($r = 0.713$, $P = 0.002$) and $p27^{Kip1}$ ($r = 0.772$, $P < 0.001$). Collectively, our results strengthened the hypothesis that miR-495 mediates G1-S arrest of breast cancer through suppression of prooncogene Bmi-1.

In Vivo Assay Reveals the Suppressive Role of miR-495 on Tumorigenicity

BALB/C nude mice were used to test and verify the above conclusion using MDA-MB-231. As shown in Figure 7A, miR-495-tranfected cells showed an anti-proliferative tendency in nude mice. Tumor volume and tumor weight generated from miR-495-transfected cells were decreased compared with that from vector-transfected cells (Figure 7B and Figure 7C). The expression of miR-495 was determined in all transplanted tumors after the mice were killed. Real-time PCR revealed miR-495 was intensively expressed in that tumors generated from miR-495-transfected MDA-MB-231 cells, but weakly expressed in the vector-transfected group (Figure 7D). Supplementation of Bmi-1 attenuated the repressive effect of miR-495 in the nude mice transplant assay. The histological statuses of these tumors were validated by H&E staining and immunohistochemical staining for Bmi-1 in the indicated excised tumors was performed (Figure 7E). As expected, Bmi-1 was decreased in the miR-495-transfected group compared with the vector-transfected group and was increased in the Bmi-1 complementary transfected cells. Taken together, our results demonstrated that Bmi-1 plays an important role in the reduced tumorigenicity induced by miR-495 in nude mice.

DISCUSSION

A report by National Cancer Institute pointed out that breast cancer will be the secondary diagnosed nonskin malignancy in US women in 2015.[41–43] Large tumor size, growing by cell proliferation, is commonly considered an established prognostic marker.[44] More and more evidence shows that gene disorders in cells deeply influence proliferation, tumorigenesis and treatment strategies.[45–47] Both loss and gain of critical genes in key pathways, especially those related to proliferation, are involved in cancer development and the selection of therapeutic strategies.[48] The AKT pathway is a critical regulatory mechanism mediated by many key gene products, such as Bmi-1,[36] NFκB,[39] Snail (snail family zinc finger 1),[40] and BCL2 (B-cell CLL/lymphoma 2).[41] In breast cancer, high Bmi-1 expression is correlated with advanced clinicopathological classifications (T, N, and M) and clinical stages.[14] Furthermore, a high level of Bmi-1 indicates an unfavorable overall survival and serves as a high risk marker for breast cancer.[14] Similarly, Hex-protein docking analysis revealed that the *Bmi-1* gene was co-regulated (down) with the progesterone receptor in invasive ductal breast carcinoma, which supported Bmi-1 as a biomarker of breast cancer.[42]

Many studies have shown that Bmi-1 plays vital roles in multiple tissues. In $Bmi\text{-}1^{-/-}$ mice, DNA damage, impaired mitochondrial structure, decreased mitochondrial numbers, and increased oxidative stress occurred.[49] When the expression of Bmi-1 was blocked by siRNA transduction, the proliferation of oral epithelial cells was inhibited and immortalized cells was decreased.[50] Endogenously inhibition of Bmi-1 reduced the invasiveness of 2 HCC cell lines in vitro by upregulating PTEN expression and inhibiting the phosphatidylinositol 3-kinase (PI3K)/Akt signaling pathway.[51] However, how Bmi-1 is regulated in breast cancer remains to be investigated. It is reasonable to expect that the expression of Bmi-1 mediated by epigenetic changes, such as miRNAs, may contribute directly to the disease progression of various cancers.

Several miRNAs are involved in the regulation of the oncogene *Bmi-1*, such as miR-200c in radiation-induced thymic lymphoma,[52] miR-15a and miR-16 in ovarian cancer,[53] miR200b in prostate cancer,[53] and miR-203 in esophageal cancer;[27] For the first time, we revealed that miR-495 was dramatically decreased in breast cancer cell lines compared with NBECs. Furthermore, we demonstrated that ectopic expression of miR-495 drastically retarded the proliferation

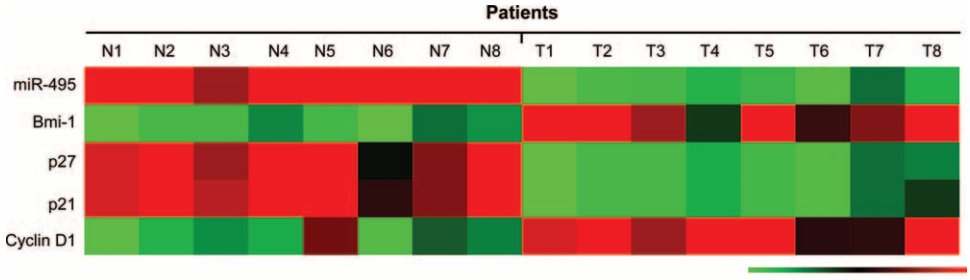

Statistical analysis of indicated genes

		Bmi-1	p21	p27	Cyclin D1
miR-495	Correlation coefficient	-0.802	0.713	0.772	-0.729
	Sig.	<0.001	0.002	<0.001	0.001

FIGURE 6. The relationship between miR-495 and Bmi-1, cyclin D1, $p21^{Cip1}$, and $p27^{Kip1}$ in 8 paired normal human breast tissues (N1–N8) and human breast cancer tissues (T1–T8). (A) Red represents higher expression and green represents lower expression tested by real-time PCR. (B) Correlation analysis between miR-495 and Bmi-1 or other indicated genes by the SPSS13.0 software. PCR = polymerase chain reaction.

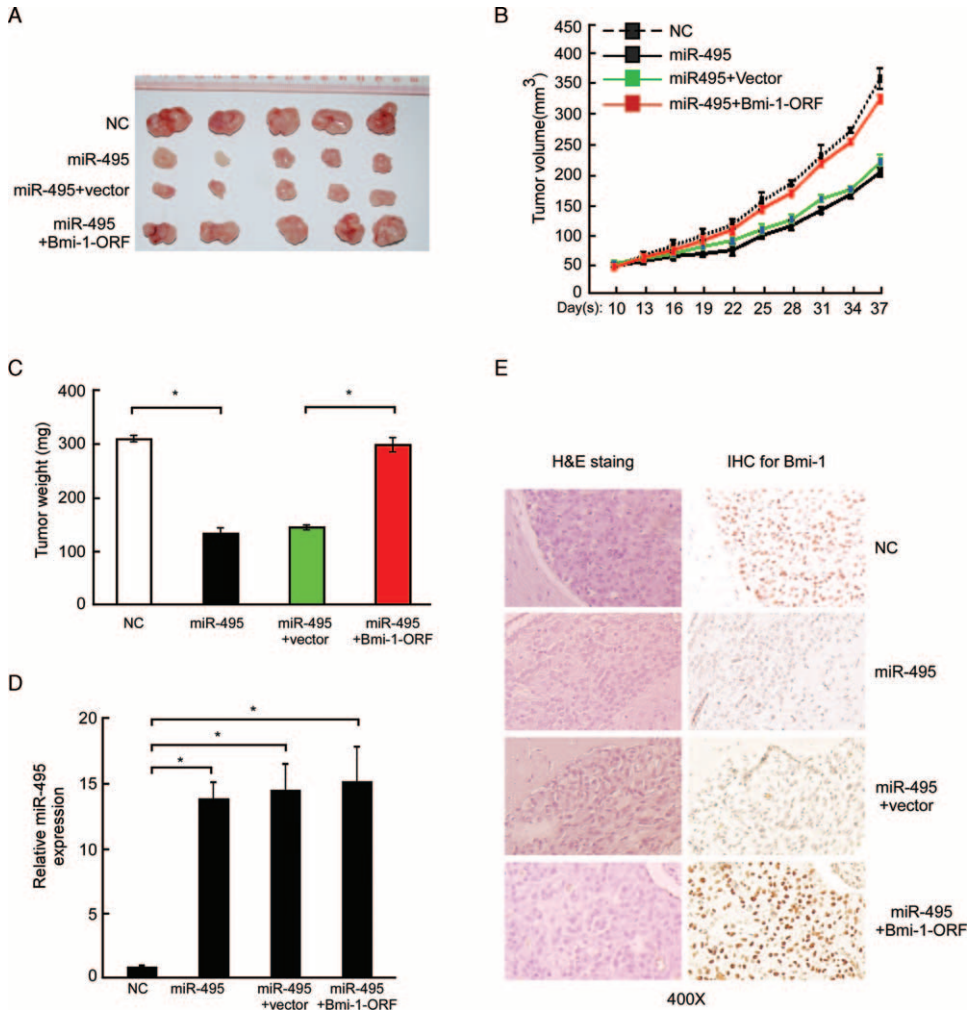

FIGURE 7. The inhibitory effect of miR-495 and the neutralizing effect of Bmi-1 on proliferation indicated by in vivo assays. (A) Images of excised tumors 37 days after injection. (B) The growth curve of tumor measured every 3 days from the beginning of the 10th day. Data are means ± standard error mean of all tumor volumes per group. (C) The weight of excised tumors measured on day 37 by electronic weighing. (D) The expression of miR-495 of indicated excised tumors as assessed by real-time PCR. (E) Hematoxylin and eosin staining (H&E staining) and immunohistochemical staining for Bmi-1 of indicated excised tumors. Three independent experiments were conducted in each assay. Error bars correspond to the mean ± standard deviation. $^{*}P < 0.05$. PCR = polymerase chain reaction.

and tumorigenicity in in vitro and in vivo assays, suggesting that downregulation of miR-495 may associate with features of breast cancer and that it functions as an antimir. Consistent with present findings in breast cancer, the expression level of miR-495 is downregulated in gastric cancer,[54] prostate cancer,[55] and non-small cell lung cancer.[56] However, it has been reported that miR-495 directly suppressed E-cadherin expression to promote cell invasion, indicating that upregulated miR-495 plays important roles in epithelial-to-mesenchymal transition (EMT), which was further confirmed by Cao et al that miR-495 could induce breast cancer cell migration.[57,58] Interestingly, Dr. Robert A. Weinberg has documented that activation of the EMT program in carcinoma cells can give rise to cells with stem-like properties.[59] Indeed, miR-495 is found to be upregulated in breast cancer stem cells.[57] Moreover, Cao et al[58] found that miR-495 also upregulated in breast cancer samples. Therefore, miR-495 might be expressed in the different levels in different subpopulation of breast cancer cells, which miR-495 is upregulated in the cancer stem cells that also showed highly invasive ability, but is downregulated in differentiated breast cancer cells that showed high proliferative rate. Our data may further confirm and explain the consistent detection that miR-495 inhibits proliferation of glioblastoma multiforme cells by downregulating CDK6.[60] Overall, these studies prompted us to investigate further the relationship between miR-495 and clinical characteristics, such as tumor, node, and metastasis in extensive clinical samples.

Why is miR-495 frequently downregulated in breast cancer? One study observed that miR-495 is upregulated by E12/E47, which prompted us to look for a regulator of miR-495.[57] By analyzing the position of miR-495 in the genome, the promoter regulatory region of miR-495 might be: chromosome 14:101,498,500–101, 500,091. The ECR browser, a tool for visualizing and accessing data from comparisons, was used to predict conserved transcription factor-binding sites in the identified region. Growth factor independent 1 transcription repressor (GFI1), known to form a large protein complex with co-repressors that recruit histone deacetylases, has 3 binding sites

in the miR-495 promoter (see supplementary Figure S1, http://links.lww.com/MD/A245). GFI1 is overexpressed and acts as a proliferation repressor in chronic myelogenous leukemia,[53] neuroendocrine lung cancer cell lines,[61] and prostate cancer cells.[62] By searching the GSE profiles, it was indicated that GFI1 is upregulated in breast cancer compared with normal breast tissue, according to profile GDS2617. Therefore, we speculated that GFI1 is a direct regulator of miR-495 and plan to verify this hypothesis in the future experiments.

Firstly, we elucidated that miR-495-mediated G1-S arrest was associated with downregulation of oncogene Bmi-1. The current findings suggest a significant biological role of miR-495 in the regulation of proliferation and tumorigenicity of breast cancer cells. Our study suggests a potential usefulness of miR-495-targeting strategies to deliver an anti-proliferative therapeutic effect.

ACKNOWLEDGMENTS

None.

REFERENCES

1. Jacobs JJ, Scheijen B, Voncken JW, et al. Bmi-1 collaborates with c-Myc in tumorigenesis by inhibiting c-Myc-induced apoptosis via INK4a/ARF. *Genes Dev.* 1999;13:2678–2690.
2. Jacobs JJ, Kieboom K, Marino S, et al. The oncogene and Polycomb-group gene bmi-1 regulates cell proliferation and senescence through the ink4a locus. *Nature.* 1999;397:164–168.
3. Fraser PE, Sauka-Spengler T. Expression of the polycomb group gene bmi-1 in the early chick embryo. *Gene Expr Patterns.* 2004;5:23–27.
4. Abd El hafez A, El-Hadaad HA. Immunohistochemical expression and prognostic relevance of Bmi-1, a stem cell factor, in epithelial ovarian cancer. *Ann Diagn Pathol.* 2014;18:58–62.
5. Jin M, Zhang T, Liu C, et al. miRNA-128 suppresses prostate cancer by inhibiting BMI-1 to inhibit tumor-initiating cells. *Cancer Res.* 2014;74:4183–4195.
6. Chiba T, Miyagi S, Saraya A, et al. The polycomb gene product BMI1 contributes to the maintenance of tumor-initiating side population cells in hepatocellular carcinoma. *Cancer Res.* 2008;68:7742–7749.
7. Ma L, Wang H, Yao H, et al. Bmi1 expression in oral lichen planus and the risk of progression to oral squamous cell carcinoma. *Ann Diagn Pathol.* 2013;17:327–330.
8. Becker M, Korn C, Sienerth AR, et al. Polycomb group protein Bmi1 is required for growth of RAF driven non-small-cell lung cancer. *PLoS One.* 2009;4:e4230.
9. Zhang XW, Sheng YP, Li Q, et al. BMI1 and Mel-18 oppositely regulate carcinogenesis and progression of gastric cancer. *Mol Cancer.* 2010;9:40.
10. Nacerddine K, Beaudry JB, Ginjala V, et al. Akt-mediated phosphorylation of Bmi1 modulates its oncogenic potential, E3 ligase activity, and DNA damage repair activity in mouse prostate cancer. *J Clin Invest.* 2012;122:1920–1932.
11. Choy B, Bandla S, Xia Y, et al. Clinicopathologic characteristics of high expression of Bmi-1 in esophageal adenocarcinoma and squamous cell carcinoma. *BMC Gastroenterol.* 2012;12:146.
12. Min L, Dong-Xiang S, Xiao-Tong G, et al. Clinicopathological and prognostic significance of Bmi-1 expression in human cervical cancer. *Acta Obstet Gynecol Scand.* 2011;90:737–745.
13. Hayry V, Tynninen O, Haapasalo HK, et al. Stem cell protein BMI-1 is an independent marker for poor prognosis in oligodendroglial tumours. *Neuropathol Appl Neurobiol.* 2008;34:555–563.
14. Guo BH, Feng Y, Zhang R, et al. Bmi-1 promotes invasion and metastasis, and its elevated expression is correlated with an advanced stage of breast cancer. *Mol Cancer.* 2011;10:10.
15. Song LB, Li J, Liao WT, et al. The polycomb group protein Bmi-1 represses the tumor suppressor PTEN and induces epithelial-mesenchymal transition in human nasopharyngeal epithelial cells. *J Clin Invest.* 2009;119:3626–3636.
16. Wang HB, Liu GH, Zhang H, et al. Sp1 and c-Myc regulate transcription of BMI1 in nasopharyngeal carcinoma. *FEBS J.* 2013;280:2929–2944.
17. Goel HL, Chang C, Pursell B, et al. VEGF/neuropilin-2 regulation of Bmi-1 and consequent repression of IGF-IR define a novel mechanism of aggressive prostate cancer. *Cancer Discov.* 2012;2:906–921.
18. Jiang L, Song L, Wu J, et al. Bmi-1 promotes glioma angiogenesis by activating NF-kappaB signaling. *PLoS One.* 2013;8:e55527.
19. Li H, Zheng D, Zhang B, et al. Mir-208 promotes cell proliferation by repressing SOX6 expression in human esophageal squamous cell carcinoma. *J Transl Med.* 2014;12:196.
20. Kozomara A, Griffiths-Jones S. miRBase: annotating high confidence microRNAs using deep sequencing data. *Nucleic Acids Res.* 2014;42:D68–73.
21. Wang Y, Melton C, Li YP, et al. miR-294/miR-302 promotes proliferation, suppresses G1-S restriction point, and inhibits ESC differentiation through separable mechanisms. *Cell Rep.* 2013;4:99–109.
22. Ma Y, Qin H, Cui Y. MiR-34a targets GAS1 to promote cell proliferation and inhibit apoptosis in papillary thyroid carcinoma via PI3K/Akt/Bad pathway. *Biochem Biophys Res Commun.* 2013;441:958–963.
23. Kim BM, Choi MY. Non-canonical microRNAs miR-320 and miR-702 promote proliferation in Dgcr8-deficient embryonic stem cells. *Biochem Biophys Res Commun.* 2012;426:183–189.
24. Li J, Zhao L, He X, et al. MiR-21 inhibits c-Ski signaling to promote the proliferation of rat vascular smooth muscle cells. *Cell Signal.* 2014;26:724–729.
25. Zhu C, Shao P, Bao M, et al. miR-154 inhibits prostate cancer cell proliferation by targeting CCND2. *Urol Oncol.* 2014;32:31e39–31e16.
26. Yu Q, Liu SL, Wang H, et al. miR-126 Suppresses the proliferation of cervical cancer cells and alters cell sensitivity to the chemotherapeutic drug bleomycin. *Asian Pac J Cancer Prev.* 2013;14:6569–6572.
27. Yu X, Jiang X, Li H, et al. miR-203 inhibits the proliferation and self-renewal of esophageal cancer stem-like cells by suppressing stem renewal factor Bmi-1. *Stem Cells Dev.* 2014;23:576–585.
28. Tu X, Zhang H, Zhang J, et al. MicroRNA-101 suppresses liver fibrosis by targeting TGFbeta signaling pathway. *J Pathol.* 2014.
29. Xie Q, Yan Y, Huang Z, et al. MicroRNA-221 targeting PI3-K/Akt signaling axis induces cell proliferation and BCNU resistance in human glioblastoma. *Neuropathology.* 2014.
30. Subramanian M, Rao SR, Thacker P, et al. MiR-29b downregulates canonical Wnt signaling by targeting BCL9L and other coactivators of beta-catenin in human colorectal cancer cells. *J Cell Biochem.* 2014.
31. Palacios F, Abreu C, Prieto D, et al. Activation of the PI3K/AKT pathway by microRNA-22 results in CLL B-cell proliferation. *Leukemia.* 2014.

32. Zhou X, Hu Y, Dai L, et al. MicroRNA-7 Inhibits Tumor Metastasis and Reverses Epithelial-Mesenchymal Transition through AKT/ERK1/2 Inactivation by Targeting EGFR in Epithelial Ovarian Cancer. *PLoS One.* 2014;9:e96718.
33. Song L, Wang L, Li Y, et al. Sam68 up-regulation correlates with, and its down-regulation inhibits, proliferation and tumourigenicity of breast cancer cells. *J Pathol.* 2010;222:227–237.
34. Lin H, Dai T, Xiong H, et al. Unregulated miR-96 induces cell proliferation in human breast cancer by downregulating transcriptional factor FOXO3a. *PLoS One.* 2010;5:e15797.
35. Song LB, Zeng MS, Liao WT, et al. Bmi-1 is a novel molecular marker of nasopharyngeal carcinoma progression and immortalizes primary human nasopharyngeal epithelial cells. *Cancer Res.* 2006;66:6225–6232.
36. Hu J, Liu YL, Piao SL, et al. Expression patterns of USP22 and potential targets BMI-1, PTEN, p-AKT in non-small-cell lung cancer. *Lung Cancer.* 2012;77:593–599.
37. Lin C, Song L, Liu A, et al. Overexpression of AKIP1 promotes angiogenesis and lymphangiogenesis in human esophageal squamous cell carcinoma. *Oncogene.* 2015;34:384–393.
38. Pathmanathan N, Balleine RL. Ki67 and proliferation in breast cancer. *J Clin Pathol.* 2013;66:512–516.
39. Shair KH, Bendt KM, Edwards RH, et al. EBV latent membrane protein 1 activates Akt, NFkappaB, and Stat3 in B cell lymphomas. *PLoS Pathog.* 2007;3:e166.
40. Okui G, Tobiume K, Rizqiawan A, et al. AKT primes snail-induced EMT concomitantly with the collective migration of squamous cell carcinoma cells. *J Cell Biochem.* 2013;114:2039–2049.
41. Drukker L, Margulis A, Chaouat M, et al. Changes of PI3K/AKT/BCL2 signaling proteins in congenital Giant Nevi: melanocytes contribute to their increased survival and integrity. *J Recept Signal Transduct Res.* 2013;33:359–366.
42. Parvathi MV, Murthy PB, Vennila M, et al. Regulation of BMI1 Polycomb gene expression in histological grades of invasive ductal breast carcinomas and its correlation with hormone receptor status. *Tumour Biol.* 2013;34:3807–3815.
43. Sestak I, Cuzick J. Update on breast cancer risk prediction and prevention. *Curr Opin Obstet Gynecol.* 2015;27:92–97.
44. Harirchi I, Azary S, Montazeri A, et al. Literacy and breast cancer prevention: a population-based study from Iran. *Asian Pac J Cancer Prev.* 2012;13:3927–3930.
45. Vickers AJ, Salz T, Basch E, et al. Electronic patient self-assessment and management (SAM): a novel framework for cancer survivorship. *BMC Med Inform Decis Mak.* 2010;10:34.
46. Jeon HY, Choi M, Howlett EL, et al. Expression patterns of astrocyte elevated gene-1 (AEG-1) during development of the mouse embryo. *Gene Expr Patterns.* 2010;10:361–367.
47. Emdad L, Lee SG, Su ZZ, et al. Astrocyte elevated gene-1 (AEG-1) functions as an oncogene and regulates angiogenesis. *Proc Natl Acad Sci U S A.* 2009;106:21300–21305.
48. Xu K, Song X, Chen Z, et al. XRCC2 promotes colorectal cancer cell growth, regulates cell cycle progression, and apoptosis. *Medicine (Baltimore).* 2014;93:e294.
49. Jin J, Lv X, Chen L, et al. Bmi-1 plays a critical role in protection from renal tubulointerstitial injury by maintaining redox balance. *Aging Cell.* 2014.
50. Qiao B, Chen Z, Hu F, et al. BMI-1 activation is crucial in hTERT-induced epithelial-mesenchymal transition of oral epithelial cells. *Exp Mol Pathol.* 2013;95:57–61.
51. Li X, Yang Z, Song W, et al. Overexpression of Bmi-1 contributes to the invasion and metastasis of hepatocellular carcinoma by increasing the expression of matrix metalloproteinase (MMP)2, MMP-9 and vascular endothelial growth factor via the PTEN/PI3K/Akt pathway. *Int J Oncol.* 2013;43:793–802.
52. Cui J, Cheng Y, Zhang P, et al. Down regulation of miR200c promotes radiation-induced thymic lymphoma by targeting BMI1. *J Cell Biochem.* 2014;115:1033–1042.
53. Huang M, Hu Z, Chang W, et al. The growth factor independence-1 (Gfi1) is overexpressed in chronic myelogenous leukemia. *Acta Haematol.* 2010;123:1–5.
54. Li Z, Cao Y, Jie Z, et al. miR-495 and miR-551a inhibit the migration and invasion of human gastric cancer cells by directly interacting with PRL-3. *Cancer Lett.* 2012;323:41–47.
55. Formosa A, Markert EK, Lena AM, et al. MicroRNAs, miR-154, miR-299-5p, miR-376a, miR-376c, miR-377, miR-381, miR-487b, miR-485-3p, miR-495 and miR-654-3p, mapped to the 14q32.31 locus, regulate proliferation, apoptosis, migration and invasion in metastatic prostate cancer cells. *Oncogene.* 2013.
56. Song L, Li Y, Li W, et al. miR-495 Enhances the Sensitivity of Non-Small Cell Lung Cancer Cells to Platinum by Modulation of Copper-Transporting P-type Adenosine Triphosphatase A (ATP7A). *J Cell Biochem.* 2014;115:1234–1242.
57. Hwang-Verslues WW, Chang PH, Wei PC, et al. miR-495 is upregulated by E12/E47 in breast cancer stem cells, and promotes oncogenesis and hypoxia resistance via downregulation of E-cadherin and REDD1. *Oncogene.* 2011;30:2463–2474.
58. Cao M, Nie W, Li J, et al. MicroRNA-495 induces breast cancer cell migration by targeting JAM-A. *Protein Cell.* 2014;5:862–872.
59. Pattabiraman DR, Weinberg RA. Tackling the cancer stem cells - what challenges do they pose? *Nat Rev Drug Discov.* 2014;13:497–512.
60. Chen SM, Chen HC, Chen SJ, et al. MicroRNA-495 inhibits proliferation of glioblastoma multiforme cells by downregulating cyclin-dependent kinase 6. *World J Surg Oncol.* 2013;11:87.
61. Kazanjian A, Wallis D, Au N, et al. Growth factor independence-1 is expressed in primary human neuroendocrine lung carcinomas and mediates the differentiation of murine pulmonary neuroendocrine cells. *Cancer Res.* 2004;64:6874–6882.
62. Dwivedi PP, Anderson PH, Tilley WD, et al. Role of oncoprotein growth factor independent-1 (GFI1) in repression of 25-hydroxyvitamin D 1alpha-hydroxylase (CYP27B1): a comparative analysis in human prostate cancer and kidney cells. *J Steroid Biochem Mol Biol.* 2007;103:742–746.